

## Supporting Information

### Two compatible polymer donors contribute synergistically for ternary organic solar cells with 17.53% efficiency

Qiaoshi An,<sup>\*‡<sup>a</sup></sup> Junwei Wang,<sup>‡<sup>b</sup></sup> Xiaoling Ma,<sup>c</sup> Jinhua Gao,<sup>c</sup> Zhenghao Hu,<sup>c</sup> Bin Liu,<sup>b</sup> Huiliang Sun,<sup>b</sup> Xugang Guo<sup>b</sup>, Xiaoli Zhang<sup>d</sup> and Fujun Zhang<sup>c</sup>

<sup>a</sup> School of Chemistry and Chemical Engineering, Beijing Institute of Technology, 100081, Beijing, China

<sup>b</sup> Department of Materials Science and Engineering, Southern University of Science and Technology, 518055, Shenzhen, China

<sup>c</sup> School of Science, Beijing Jiaotong University, 100044, Beijing, China

<sup>d</sup> State Centre for International Cooperation on Designer Low-Carbon & Environmental Materials, School of Materials Science and Engineering, Zhengzhou University, 450001, Zhengzhou, China

\*Correspondence: qsan@bit.edu.cn

‡ The two authors contributed equally to this work

#### 1. Detailed experimental section

##### Materials

PDIN (Lot# WJ425A), PM6 (Lot# ZJ415B), Y6 (Lot# YJ319A) were purchased from Solarmer Materials Inc and used as received. The number-average molecular weight ( $M_n$ ) of the PM6 offered by the company is about 30 kDa, and the polydispersity index (PDI) is around 2.3. S3 was synthesized based on Moon's pioneer work<sup>1</sup> and our previous work<sup>2, 3</sup>. The corresponding  $M_n$  of the S3 is about 37.5 kDa, and PDI is around 2.1. PEDOT:PSS (clevios P VP Al 4083) was purchased from H.C. Starck co. Ltd.

##### OSCs fabrication and measurement

The patterned indium tin oxide (ITO) glass coated substrates (sheet resistance  $15 \Omega/\square$ ) were consecutively cleaned in ultrasonic baths containing detergent, de-ionized water and ethanol, respectively. Then, poly-(3,4-ethylenedioxythiophene):poly-(styrenesulphonic acid) (PEDOT:PSS) thin films were fabricated on the cleaned ITO substrates by spin-coating method at 5000 round per minute (RPM) for 40 s, and then annealed at  $150^\circ\text{C}$  for 10 minutes in ambient conditions. After annealing treatment, the ITO substrates coated PEDOT:PSS films were transferred to a high-purity nitrogen-filled glove box to fabricate active layers. The used materials PM6, Y6 and S3 were dissolved in chloroform (CF) with the solvent additive of 1-chloronaphthalene (CN) (0.5%, v/v) to prepare  $17.6 \text{ mg ml}^{-1}$  blend solutions. The weight ratios of PM6 to S3 are 1:0, 0.9:0.1, 0.8:0.2, 0.7:0.3, 0.5:0.5, 0:1 and the weight ratio of donor(s) to acceptor is kept constant as 1:1.2. The blend solutions were spin-coated on PEDOT:PSS films in a high purity nitrogen-filled glove box to fabricate the active layers. The active layers were solvent vapor annealed with carbon disulfide for 30 s and then annealed at  $80^\circ\text{C}$  for 5 min. The optimized thickness of the active layer is  $\sim 100 \text{ nm}$ , which was measured by Ambios Technology XP-2 stylus Profiler. After that, PDIN solution ( $2 \text{ mg ml}^{-1}$  in methanol with 0.25 vol% acetic acid) was spin-coated on the top of active layers at 5000

RPM for 30 s. The cathode of Al was deposited by thermal evaporation with a shadow mask under  $10^{-4}$  Pa and the thickness of 100 nm was monitored by a quartz crystal microbalance. The active area of OSCs is about  $3.8 \text{ mm}^2$ , which is defined by the overlap of ITO anode and Al cathode.

### **Characterizations on films and OSCs**

The ultraviolet-visible (UV-Vis) absorption spectra of pure PM6, S3 and Y6 films were obtained using a Shimadzu UV-3101 PC spectrometer. The electrochemical cyclic voltammetry (CV) was conducted on an electrochemical workstation (CHI660D Chenhua Shanghai) with Pt plate as working electrode. The current-voltage (I-V) curves of all OSCs were measured in a high-purity nitrogen-filled glove box using a Keithley 2400 source meter. AM 1.5G irradiation at  $100 \text{ mW cm}^{-2}$  provided by An XES-40S2 (SAN-EI Electric Co., Ltd.) solar simulator (AAA grade,  $70 \times 70 \text{ mm}^2$  photobeam size), which was calibrated by standard silicon solar cells (purchased from Zolix INSTRUMENTS CO. LTD). The external quantum efficiency (EQE) spectra of OSCs were measured in air conditions by a Zolix Solar Cell Scan 100.

### **AFM and TEM**

The morphology of the active layers was investigated by AFM using a Dimension Icon AFM (Bruker) in a tapping mode. TEM images of the active layers were obtained by using a JEOL JEM-1400 transmission electron microscope operated at 80 kV. The samples for AFM and TEM characterization were prepared under the same conditions compared with the active layers of the OSCs. The samples for TEM measurement were prepared by dissolving the PEDOT:PSS layer using deionized water and picked up the active layer using 400-mesh copper TEM grids.

### **GIWAXS**

The GIWAXS characterization with samples were performed at BL16B1 beamline of Shanghai Synchrotron Radiation Facility. The samples were prepared under the same conditions of the OSCs on the Glass/PEDOT:PSS substrates. The wavelength of incident X-ray was 0.124 nm and the exposure time of samples was 60 s. The incidence light angle of X ray was  $0.12^\circ$  and the scattering signal was collected by mar165CCD with a pixel size of 0.172 mm by 0.172 mm. The GIWAXS was done in air environment, and the sample-to-detector distance was  $\approx 252 \text{ mm}$  (calibrated by AgB sample).

### **Charge mobility measurement by SCLC method**

The structure of electron-only devices is ITO/ZnO/active layer/PDIN/Al and the structure of hole-only devices is ITO/PEDOT:PSS/active layer/MoO<sub>3</sub>/Ag. The fabrication conditions of the active layer films are same with those for the OSCs. The charge mobilities are generally described by the Mott-Gurney equation<sup>4-6</sup>:

$$J = \frac{9}{8} \varepsilon_r \varepsilon_0 \mu \frac{V^2}{L^3} \quad (1)$$

where  $J$  is the current density,  $\varepsilon_0$  is the permittivity of free space ( $8.85 \times 10^{-14} \text{ F/cm}$ ),  $\varepsilon_r$  is the dielectric constant of used materials,  $\mu$  is the charge mobility,  $V$  is the applied voltage and  $L$  is the

active layer thickness. The  $\epsilon_r$  parameter is assumed to be 3, which is a typical value for organic materials. In organic materials, charge mobility is usually field dependent and can be described by the disorder formalism, typically varying with electric field,  $E=V/L$ , according to the equation<sup>7-9</sup>:

$$\mu = \mu_0 \exp\left[0.89\gamma\sqrt{\frac{V}{L}}\right] \quad (2)$$

where  $\mu_0$  is the charge mobility at zero electric field and  $\gamma$  is a constant. Then, the Mott-Gurney equation can be described by:

$$J = \frac{9}{8} \epsilon_r \epsilon_0 \mu_0 \frac{V^2}{L^3} \exp\left[0.89\gamma\sqrt{\frac{V}{L}}\right] \quad (3)$$

In this case, the charge mobilities were estimated using the following equation:

$$\ln\left(\frac{JL^3}{V^2}\right) = 0.89\gamma\sqrt{\frac{V}{L}} + \ln\left(\frac{9}{8} \epsilon_r \epsilon_0 \mu_0\right) \quad (4)$$

### EL Measurement

An external current/voltage source was employed to provide an external electric field to the pristine and blended solar cells. The electroluminescence emissions were recorded with an Andor spectrometer.

### Highly sensitive EQE and EQE<sub>EL</sub> Measurement

Highly sensitive EQE was measured using an integrated system (PECT-600, Enlitech), where the photocurrent was amplified and modulated by a lock-in instrument. EQE<sub>EL</sub> measurements were performed by applying external voltage/current sources through the OSCs (ELCT-3010, Enlitech). All of the OSCs were prepared for EQE<sub>EL</sub> measurements according to the optimal device fabrication conditions.

## 2. Additional experimental results

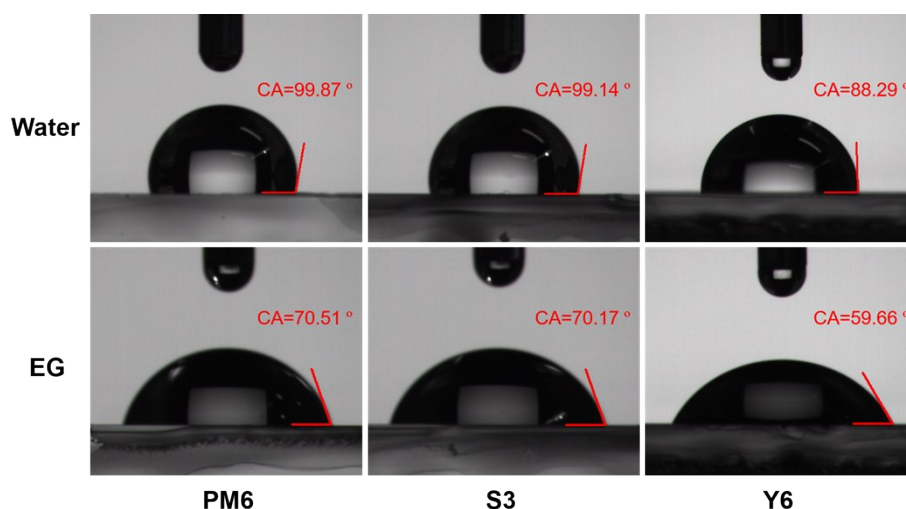
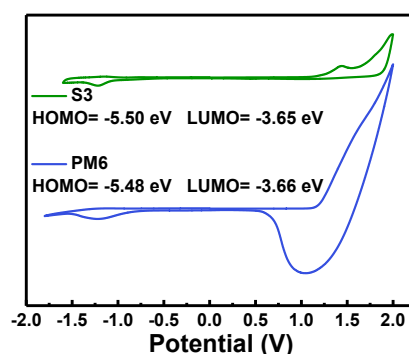
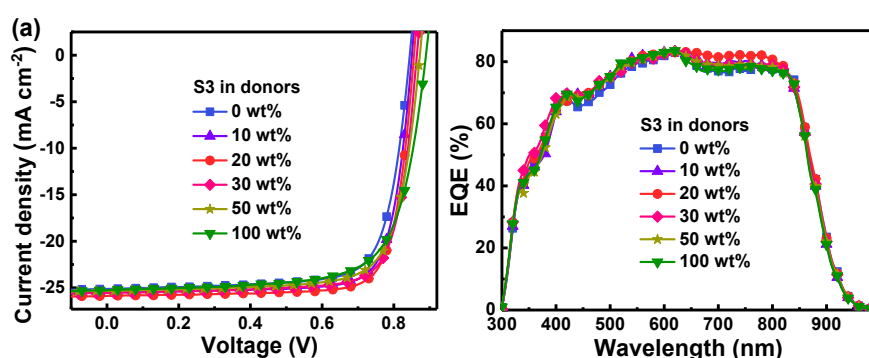


Figure S1. The contact angle images of pure PM6, S3 and Y6 films.

**Table S1.** Contact angle, surface tension and interfacial tension ( $\gamma$ ) of individual materials,

X	Water contact angle [°]	EG contact angle [°]	$\gamma^d$ [mN m <sup>-1</sup> ]	$\gamma^p$ [mN m <sup>-1</sup> ]	Surface tension [mN m <sup>-1</sup> ]	$\gamma_{PM6-X}$ [mN m <sup>-1</sup> ]	$\gamma_{S3-X}$ [mN m <sup>-1</sup> ]
PM6	99.87	70.51	28.76	0.51	29.2	-	0.05
S3	99.14	70.17	28.15	0.66	28.8	0.05	-
Y6	88.29	59.66	27.28	3.36	30.6	2.03	1.78

The HOMO levels of the two donors are calculated from the onset oxidation potentials ( $E_{ox}$ ) with equation:  $E_{HOMO} = -e[(E_{ox} - E_{Fc+/Fc}) + 4.8V]$ . The LUMO levels are calculated according to  $E_{LUMO} = E_{HOMO} + E_g$ . As shown in **Figure S2**, the HOMO levels of PM6 and S3 are about -5.48 eV and -5.50 eV, respectively. The slightly lower HOMO energy level of S3 is beneficial to realize higher  $V_{OCs}$  for ternary OSCs in comparison to that of PM6-based binary cells.

**Figure S2.** CV curves of PM6 and S3 neat films, the scan rate was 50 mV/s in 0.1 M *n*-Bu<sub>4</sub>NPF<sub>6</sub> acetonitrile solution.**Figure S3** (a)  $J$ - $V$  curves of OSCs with various S3 content in donors under AM 1.5 G illumination at intensity of 100 mW cm<sup>-2</sup>. (b) The EQE spectra of the corresponding OSCs.

**Table S2** The photovoltaic parameters of 30 ternary OSCs with 20 wt% S3.

NO.	$J_{sc}$ [mA cm <sup>-2</sup> ]	FF [%]	$V_{oc}$ [V]	PCE [%]	NO.	$J_{sc}$ [mA cm <sup>-2</sup> ]	FF [%]	$V_{oc}$ [V]	PCE [%]
1	25.86	0.856	79.17	17.53	16	25.81	0.860	78.22	17.36
2	26.02	0.856	78.67	17.52	17	25.79	0.859	78.36	17.36
3	25.83	0.855	79.25	17.50	18	25.80	0.858	78.34	17.34
4	25.90	0.853	79.21	17.50	19	25.84	0.854	78.58	17.34
5	25.90	0.858	78.61	17.47	20	25.64	0.857	78.92	17.34
6	25.83	0.856	78.96	17.46	21	25.85	0.855	78.42	17.33
7	26.04	0.859	78.03	17.45	22	25.61	0.853	79.31	17.33
8	25.76	0.854	79.31	17.45	23	25.62	0.854	79.10	17.31
9	25.88	0.855	78.83	17.44	24	25.89	0.856	78.00	17.29
10	25.74	0.856	79.08	17.42	25	25.75	0.856	78.35	17.27
11	25.95	0.857	78.33	17.42	26	25.72	0.853	78.69	17.27
12	25.92	0.858	78.29	17.41	27	25.69	0.857	78.41	17.26
13	25.86	0.859	78.37	17.41	28	25.71	0.856	78.43	17.26
14	25.77	0.859	78.58	17.39	29	25.80	0.854	78.26	17.24
15	25.75	0.859	78.63	17.39	30	25.62	0.856	78.58	17.23

**Table S3** Key parameters of the typical OSCs

S3 content [ wt%]	$J_{sat}$ [mA cm <sup>-2</sup> ]	$J_{ph}^*$ [mA cm <sup>-2</sup> ]	$J_{ph}^\&$ [mA cm <sup>-2</sup> ]	$J_{ph}^*/J_{sat}$ [%]	$J_{ph}^\&/J_{sat}$ [%]
0	26.24	25.13	23.02	95.77	87.73
20	26.75	25.86	24.28	96.67	90.76
100	26.52	25.26	22.92	95.25	86.42

$J_{sat}$ : The  $J_{ph}$  under condition of  $V_{eff}=4$  V

$J_{ph}^*$ : The  $J_{ph}$  under short circuit conditions

$J_{ph}^\&$ : The  $J_{ph}$  under maximum power output conditions

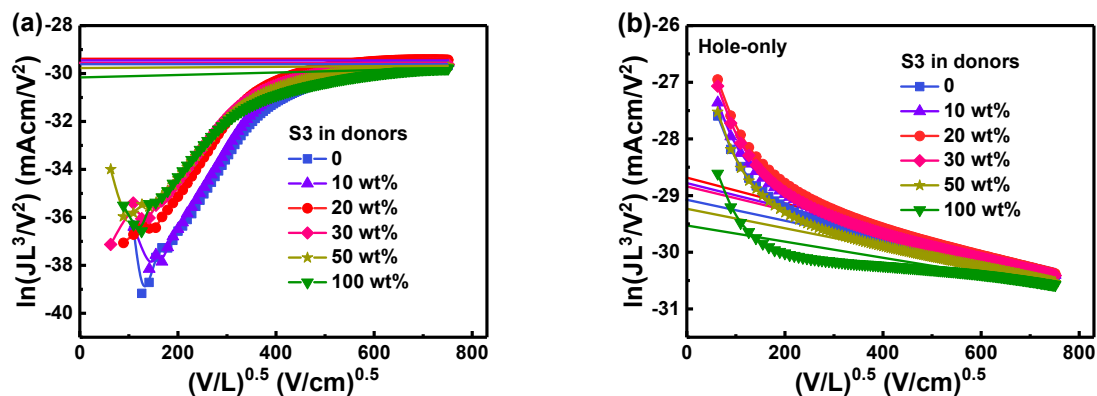


**Figure S4** The  $\ln(JL^3/V^2)$  vs  $(V/L)^{0.5}$  curves of (a) electron-only ITO/ZnO/active layer/PDIN/Al devices and (b) hole-only ITO/PEDOT:PSS/active layer/MoO<sub>3</sub>/Ag devices.

**Table S4** The electron mobility ( $\mu_e$ ), hole mobility ( $\mu_h$ ) values of the active layers with various S3 content.

S3 content [ wt%]	$\mu_e$ [cm <sup>2</sup> V <sup>-1</sup> s <sup>-1</sup> ] Avg.±Dev. <sup>a)</sup>	$\mu_h$ [cm <sup>2</sup> V <sup>-1</sup> s <sup>-1</sup> ] Avg.±Dev. <sup>a)</sup>
0	$4.33\pm 0.27\times 10^{-4}$	$7.41\pm 0.32\times 10^{-4}$
10	$4.99\pm 0.33\times 10^{-4}$	$1.01\pm 0.04\times 10^{-3}$
20	$5.68\pm 0.25\times 10^{-4}$	$1.10\pm 0.05\times 10^{-3}$
30	$4.58\pm 0.39\times 10^{-4}$	$9.32\pm 0.35\times 10^{-4}$
50	$3.82\pm 0.18\times 10^{-4}$	$6.38\pm 0.29\times 10^{-4}$
100	$2.27\pm 0.33\times 10^{-4}$	$4.67\pm 0.29\times 10^{-4}$

<sup>a)</sup>Average (Avg.) mobility values and the deviations (Dev.) based on individual 10 cells

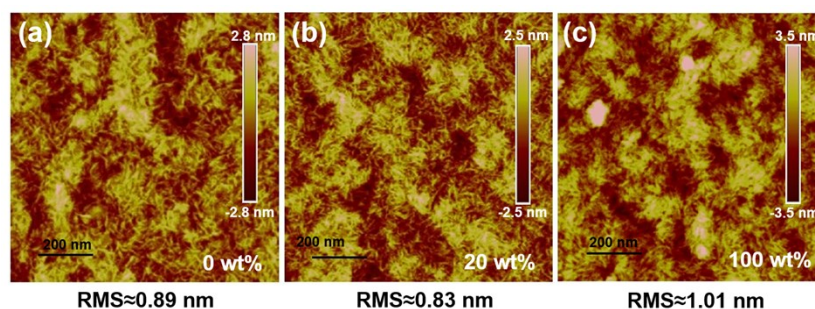


**Figure S5.** AFM height images of blend films with (a) 0 wt%, (b) 20 wt%, (c) 100 wt% S3 in donors.

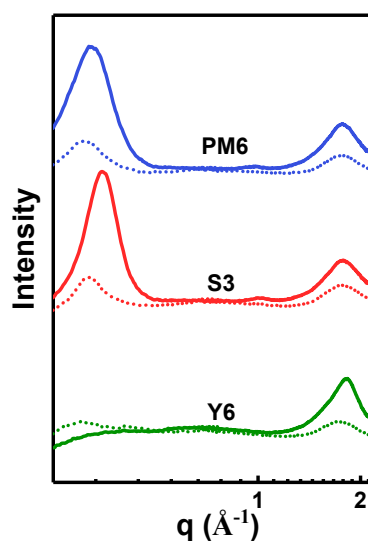


**Figure S6.** Out-of-plane (solid lines) and in-plane (dotted lines) line-cut profiles of GIWAXS.

1. S. J. Jeon, Y. W. Han and D. K. Moon, *Small*, **2019**, 15, 1902598.
2. Q. Liao, H. Sun, B. Li and X. Guo, *Sci. Bull.*, **2019**, 64, 1747.

3. H. Sun, T. Liu, J. Yu, T. K. Lau, G. Zhang, Y. Zhang, M. Su, Y. Tang, R. Ma, B. Liu, J. Liang, K. Feng, X. Lu, X. Guo, F. Gao and H. Yan, *Energy Environ. Sci.*, **2019**, 12, 3328.
4. H. Cha, D. S. Chung, S. Y. Bae, M. J. Lee, T. K. An, J. Hwang, K. H. Kim, Y. H. Kim, D. H. Choi, C. E. Park, *Adv. Funct. Mater.* **2013**, 23, 1556.
5. S. Y. Chang, H. C. Liao, Y. T. Shao, Y. M. Sung, S. H. Hsu, C. C. Ho, W. F. Su, Y. F. Chen, *J. Mater. Chem. A*. **2013**, 1, 2447.
6. Y. Zhang, D. Deng, K. Lu, J. Zhang, B. Xia, Y. Zhao, J. Fang, Z. Wei, *Adv. Mater.* **2015**, 27, 1071.
7. Z. S. An, J. S. Yu, S. C. Jones, S. Barlow, S. Yoo, B. Domercq, P. Prins, L. D. A. Siebbeles, B. Kippelen, S. R. Marder, *Adv. Mater.* **2005**, 17, 2580.
8. M. Koppe, H. J. Egelhaaf, G. Dennler, M. C. Scharber, C. J. Brabec, P. Schilinsky, C. N. Hoth, *Adv. Funct. Mater.* **2010**, 20, 338.
9. Y. X. Chen, X. Zhang, C. L. Zhan, J. N. Yao, *ACS Appl. Mater. Interfaces*. **2015**, 7, 6462.